

The Riverine Organism Drift Imager: A new technology to study organism drift in rivers and streams

Frédéric de Schaetzen¹  | Mikko Impiö²  | Basil Wagner³ | Patryk Nienaltowski¹  | Michael Arnold¹ | Martin Huber⁴ | Matthias Meyer³ | Jenni Raitoharju⁵  | Luiz G. M. Silva¹  | Roman Stocker¹ 

¹Department of Civil, Environmental and Geomatic Engineering, Institute of Environmental Engineering, ETH Zurich, Zurich, Switzerland

²Programme for Environmental Information, Finnish Environment Institute, Helsinki, Finland

³Ecology Unit, Kraftwerke Oberhasli AG, Innertkirchen, Switzerland

⁴Department of Civil, Environmental and Geomatic Engineering, ETH Zurich, Zurich, Switzerland

⁵Faculty of Information Technology, University of Jyväskylä, Jyväskylä, Finland

Correspondence

Frédéric de Schaetzen
Email: fdeschae@ethz.ch

Roman Stocker
Email: romanstocker@ethz.ch

Handling Editor: Brenda Pracheil

Abstract

1. Drift or downstream dispersal is a fundamental process in the life cycle of many riverine organisms. In the face of rapidly declining freshwater biodiversity, there is a need to enhance our capacity to study the drift of riverine organisms, by overcoming the limitations of traditional labour-intensive sampling methods that result in data of low temporal and spatial resolution.
2. To address this need, we developed a new technology, the Riverine Organism Drift Imager (RODI), which combines in situ imaging with machine-learning classification. This technique expands on the traditional methodology by replacing the collection cup of a drift net with a camera system that continuously images riverine organisms as they drift through the device. After being imaged, organisms are released into the environment unharmed. A machine-learning classifier is used after field sampling to identify drifting organisms. Therefore, RODI provides a non-invasive sampling method that can quantify organism drift at unprecedented temporal resolution.
3. Multiple deployments have served to validate the performance of the technology in the field. In its current implementation, images are captured continuously for 1.5 h at 50 frames per second. We demonstrate that the quality of the resulting images enables a convolutional neural network classifier to identify organisms to the family level. The weighted F1 score, a metric for the performance of the classifier, was 94%, based on training and testing on a field-collected dataset consisting of 4598 images of 285 organisms belonging to seven classes (one species, five families and one order).
4. In conclusion, this work provides a proof of concept, demonstrating the viability of the deployment of RODI as an automated, in situ organism drift sampler. This novel approach offers the possibility to advance our fundamental understanding of the drift of riverine organisms and how this is affected by human impacts in natural streams while, at the same time, can serve as a cost-effective tool for biodiversity monitoring.

This is an open access article under the terms of the [Creative Commons Attribution](https://creativecommons.org/licenses/by/4.0/) License, which permits use, distribution and reproduction in any medium, provided the original work is properly cited.

© 2023 The Authors. *Methods in Ecology and Evolution* published by John Wiley & Sons Ltd on behalf of British Ecological Society.

KEYWORDS

benthic invertebrates, computer vision, fish, machine learning, monitoring, neural network, rivers, streams

1 | INTRODUCTION

In river ecosystems, drift or downstream dispersal is a fundamental part of the life cycle of many fish (Lechner et al., 2016; Pavlov & Mikheev, 2017) and benthic invertebrates (Brittain & Eikeland, 1988). The drift of eggs or fish larvae provides the means to disperse from spawning or nursery habitats to suitable rearing habitats (Pavlov, 1994). Due to the specific environmental needs of fish larvae, early life-stage survival, and hence population recruitment, is dependent upon drift (Humphries et al., 2020).

Benthic invertebrate drift is an essential trophic pathway in river ecosystems. The drift of benthic invertebrates can be a process of individual microhabitat selection to optimise resource acquisition or to avoid predation (Naman et al., 2016). At the same time, entering drift increases the risk of being predated by drift-feeding specialised guilds of fish (Grossman, 2014). Therefore, the biomass and species diversity of drifting benthic invertebrates can be considered indicators of the productive capacity of streams and rivers to support fish populations (Naman et al., 2016).

Human activity, including the construction of barriers, pollution and artificial flow alterations, has significantly altered the environmental conditions experienced by many riverine organisms, leading to drastic declines in freshwater invertebrate and fish populations over the last decades (Albert et al., 2021; Deinet et al., 2020). In Switzerland, for example, 65% of all fish species are threatened or have become regionally extinct, and so are 50% of benthic invertebrate species belonging to the orders of mayflies (Ephemeroptera), stoneflies (Plecoptera) and caddisflies (Trichoptera; FOEN, 2022). To improve freshwater biodiversity management and minimise the negative impacts of human activity, it is vital to enhance our capacity to monitor aquatic biota, particularly through non-invasive, broadly deployable methods that generate data with the appropriate temporal and taxonomic resolution. More specifically, long-term (months to years) and continuous (hourly to daily) data on species presence, abundance, and movement patterns. Such approaches have been increasingly applied in terrestrial (Zwerts et al., 2021) and marine environments (Francescangeli et al., 2023) with innovative imaging systems, but are still scant in freshwater ecosystems (Struthers et al., 2015).

Riverine organism drift has, to date, been studied predominantly using drift nets (Brittain & Eikeland, 1988; Lechner et al., 2016), most commonly in wadeable streams and rivers or from boats or bridges. Drift nets work by guiding organisms into a collection cup. Sampled organisms are collected from the cup at regular intervals, usually 15 min to 3 h, and preserved (i.e. killed) for post-processing (Elliott, 1970). This is an invasive, labour-intensive process, especially for long-term studies, further complicated by the fact that invertebrate and fish drift densities peak at night (Brittain & Eikeland, 1988;

Elliott, 1970; Pavlov & Mikheev, 2017). Nets, moreover, integrate organisms over time and distances because it pools all individuals in the same sampling cup for a specific exposure time, resulting in low sample resolution (Lechner et al., 2016), hindering our capacity to temporally resolve (second or minute scale) drift patterns at the individual level (Naman et al., 2016). The post-processing step compounds this bottleneck as the taxonomic identification of the organism samples is very time-consuming and requires specialised expertise, a skill that has been declining globally (Hopkins & Freckleton, 2002). As a result, data on organism drift remains sparse, consisting only of limited measurement campaigns of low temporal resolution.

Recent advances in camera and machine-learning technologies have enabled novel image-based methods, which provide vast amounts of data and enable ecologists to study organisms cost-effectively and non-invasively (Høye et al., 2021; Lürig et al., 2021). Machine-learning-based identification methods for benthic invertebrates are well established (Årje et al., 2020; Høye et al., 2022; Lytle et al., 2010; Raitoharju et al., 2018). However, they rely on preserved organisms to allow detailed image generation in laboratory conditions, and hence depend on labour-intensive, net-based sampling. In situ imaging has the potential to streamline this process, yet to date, systems developed to study riverine organisms have focussed on larger fish (Castañeda et al., 2020; Holter et al., 2020). A system that can image and identify smaller organisms (in the mm to cm range) in rivers has been lacking.

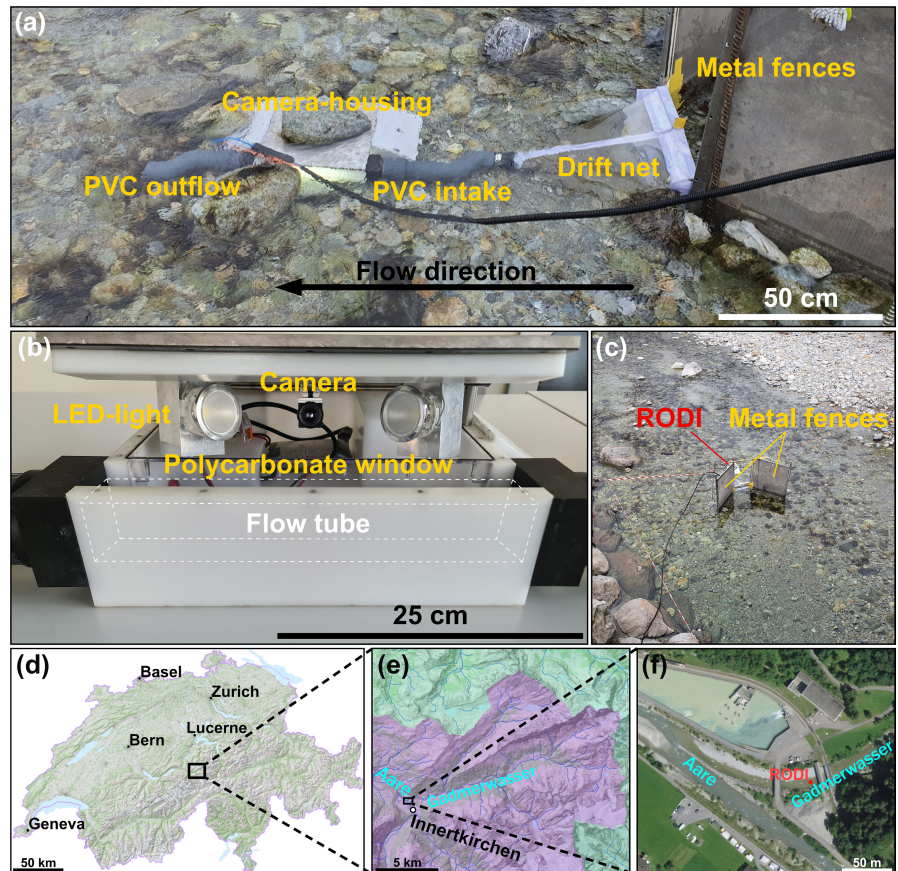
To overcome the limitations of traditional drift-net sampling, we are developing an underwater imaging system called the Riverine Organism Drift Imager (RODI). RODI provides a non-invasive, field-going, flow-through sampling method that images drifting organisms and uses a machine-learning classifier to provide taxonomic identification of imaged individuals. By continuously imaging over time, the number of drifting organisms belonging to each of a set of classes can thus be quantified with high temporal resolution and reduced effort. Here, we describe a proof of concept for RODI's technology, including the field deployments used for testing and the machine-learning approach to classify imaged organisms.

2 | MATERIALS AND METHODS

2.1 | Imaging system

Riverine Organism Drift Imager replaces the collection cup at the end of a traditional drift net with a camera system (Figure 1a; Figure S1). A net (Figure S2, mesh size 500 µm) funnels drifting organisms through a PVC tube (Figure S4) into a flow tube with a square cross-section of 50 × 50 mm (Figure 1b; Figure S3). Through

FIGURE 1 Field deployment of the Riverine Organism Drift Imager (RODI). (a) RODI installed in the riverbed and kept in place with boulders. The black arrow indicates the flow direction. (b) RODI's camera housing. Drifting organisms are guided through the flow tube (white dashed outline), where a colour camera takes multiple images of each organism in rapid sequence through a polycarbonate window. High-intensity LED lights provide sufficient light to avoid motion blur. (c) RODI in place within the river bed behind the two metal fences. The area upstream was fenced off with red–white tape to protect brown trout spawning habitats and to prevent the induction of organism drift by human activity. (d–f) The deployment location in Switzerland (46°42′28.2″ N 8°13′33.3″ E). The Gadmerwasser stream (e) is an alpine tributary of the Aare River. RODI was installed 200m upstream of the Gadmerwasser's confluence with the Aare (f).



a polycarbonate window in the flow tube, a 1920 × 1200 pixel colour camera (Teledyne-FLIR BFS-U3-23S3C-C; Teledyne FLIR LLC), installed in a purpose-built camera housing, images the flowing water and any drifting organisms at 50 frames per second. This frame rate typically yields multiple images of each drifting organism (with the number of images determined by the flow velocity). Two continuously operating LED lights (CREE CXB1512, CreeLED Inc.; Cool white 6500K, 2033 lumen) inside the camera housing provide sufficient light to operate the camera with an exposure time of only 49 μs. This fast exposure time reduces movement blurriness for drift velocities up to 2 m s⁻¹. The LED lights and camera are attached to the aluminium lid of the camera box (Figure 1b; Figure S5), allowing heat to dissipate into the surrounding water. The camera is equipped with a 12 mm objective (Edmund Optics, 12 mm UC Series fixed focal length lens, f/8 to f/11) and is installed at a working distance of 170 mm (Figure S5), resulting in a field of view of 100 mm × 61 mm and a depth of field of 35 mm. The camera housing is powered and operated by a weatherproof land station (Figure S1) that houses a laptop collecting images from the camera and a transformer (Meanwell LPC-35-1400, 24 V, 1400 mA output) for the LED lights. The land station is connected to the camera box through two cables—a USB 3.1 cable and a 2 × 1 mm² power cable, of length 15 m—combined within a flexible plastic protective sleeve. RODI operates from the regular power grid (230 V). The design plans, parts use, and construction process are described in Appendix S1.

2.2 | Field deployments

Deployments were performed in March, April and May 2022 in the lower part of the Gadmerwasser stream (Switzerland), approximately 200 m upstream of its confluence with the Aare River (Figure 1c–f). The Gadmerwasser has a managed minimum residual flow of 350 L s⁻¹ at the deployment site (Schweizer et al., 2012). The river substrate is predominantly a mix of gravel (2.5–25 mm in size) and cobbles (25–250 mm), with scattered larger boulders (>250 mm; Figure 1c). RODI was installed on the river substrate in a water depth of 20 cm by weighing it down with boulders. Upstream, two perforated metal fences (with 1.5 mm-diameter holes; Meyer et al., 2019) directed drifting organisms towards the drift net (Figure 1a,c), which was attached to the metal fences using water-resistant tape. The March deployments focused on general testing and hardware optimisation.

On 5 April 2022, freshly hatched (less than 1 day old) brown trout fry (*Salmo trutta*) were collected and released in the area between the metal fences, eventually drifting downstream through the system to be imaged. A night deployment from 10 May 2022, 21:00 until 11 May 2022, 04:30 was performed to test the system's capacity to sample naturally drifting organisms. Finally, on 11 May from 10:00 to 14:00, benthic invertebrates were systematically released into the drift net. For this trial, we collected local benthic invertebrates by dipping large river boulders in buckets containing river water to release attached invertebrates. Collected invertebrates were carefully divided on-site into classes of likeness (i.e. similar body morphology,

size and colouring). Sampled invertebrates were then released individually within the drift net and captured upon exiting. Several random organisms per likeliness class were preserved for taxonomic identification. Using a stereomicroscope (Nikon SMZ-U zoom 1:10) and taxonomic keys (Bauernfeind & Humpesch, 2001; Waringer & Graf, 2013; Zwick, 2004), these organisms were identified to the following taxonomical groups (order, family): Ephemeroptera, Heptageniidae and Baetidae; Plecoptera, Perlodidae and Capniidae; Trichoptera, Rhyacophilidae. We used data from the 5 April 2022 and 11 May 2022 (daytime) experiments to generate an annotated image dataset to be used with the machine-learning classifier. Data from the natural drift experiment, 10 May 2022, were identified by a human and were not analysed using the machine-learning classifier (described in more detail below). Lastly, in agreement with the local wildlife authority (Fishereinspektorat Kanon Bern), a permit was not required to run these experiment.

2.3 | Data acquisition and processing

Data acquisition entails the capturing of images by RODI's camera, while during processing, bounding boxes of drifting organisms or objects are extracted from each image (Figure 2). Data acquisition and processing are performed using in-house developed command-based programs compiled in C++ (Visual Studio 2015; Microsoft). The camera streams 8-bit images (BayerRG8 format) to the laptop on land, where they are saved as binary data in temporary backup files (.tmp), each file containing 1000 images (20s at 50fps, equating to 2.14GB). The hard-drive capacity of the laptop defines the duration of each data acquisition interval, which for experiments to date was 1.5h (578GB). At the end of an acquisition interval, data are transferred to an external hard drive to enable a new acquisition interval.

During data processing, the bounding box of each drifting organism or object is determined, that is, a region is defined within the image that contains the organism or object of interest so that it (and not the whole image) can subsequently be used for classification (Figure 2a). Bounding box extraction consists of several steps. The first temporary backup file (i.e. the first 1000 frames) from a given acquisition interval is converted into a video with a conventional video format (.avi). Next, using Fiji (Schindelin et al., 2012), a median background frame is calculated using the first 20 frames of the video.

The extraction of bounding boxes uses several OpenCV functions (Bradski, 2000), hereafter described as `cv::function`. For each frame in an acquisition interval, the absolute difference (`cv::absdiff`) with respect to the median background is calculated to remove stationary objects and minimise camera noise. Next, a Gaussian blur filter (`cv::blur`; 3×3 kernel size) is applied to reduce pixel noise. The resulting frame is binarised (`cv::threshold`), transforming all objects into white pixel regions, which are then saved as vectors of points (`cv::findContours`). The area of each object is calculated (`cv::contourArea`), and an area threshold is applied (typically, 2 mm^2) to remove

noise and very small objects, such as individual sediment grains. The vector of points for each object that is retained is transformed into a polygon (`cv::approxPolyDP`), around which an initial tight-fitting, rectangular bounding box (`cv::boundingRect`) is generated.

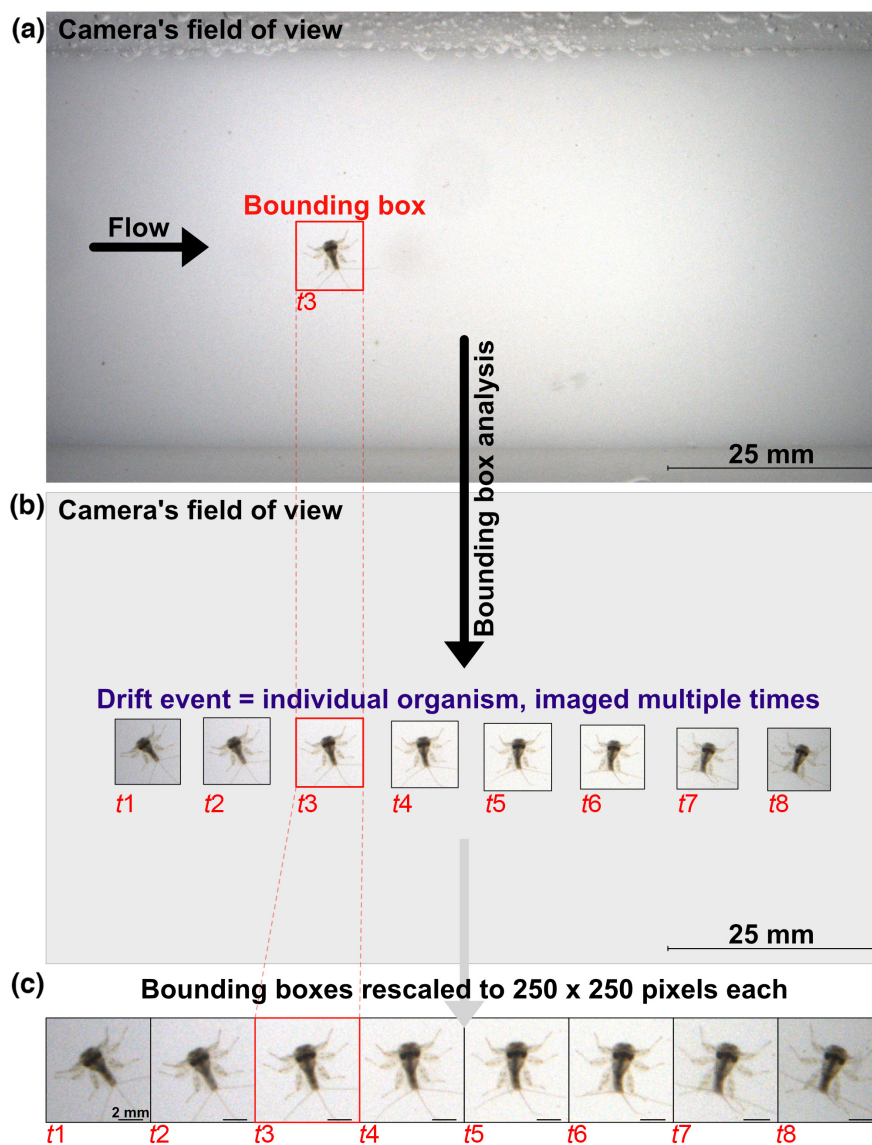
The coordinates and size of this tight-fitting, rectangular bounding box are used to define a loose-fitting, square bounding box, with each side equal to 1.5 times the longest side of the tight-fitting, rectangular bounding box. Finally, the square bounding boxes are extracted from the original raw image and saved as individual TIF files. Each drifting organism or object is imaged multiple times (typically, 10–15 times in the experiments described here) upon drifting through RODI, generating an equal number of bounding boxes. The ensemble of all bounding boxes belonging to an individual organism or object will be referred to as a 'drift event' hereafter (Figure 2b). Bounding boxes are sorted (currently this occurs manually) to retain drift events of interest, here drifting organisms, and discard other drift events (e.g. debris or air bubbles). Each drift event of interest is then given a unique identifier. Finally, all bounding boxes are converted to PNG format with a resolution of 250×250 pixels (Figures 2c and 3) in order to be used in the machine-learning classifier. The code to acquire images in the field and generate bounding boxes during processing can be found in Appendix S1.6.

2.4 | Machine-learning classifier

The bounding boxes extracted from in situ acquired images (Figure 3) form the input of a machine-learning classifier. For the classification process, an annotated dataset was obtained from the images recorded in the experiments on 5 April 2022 (brown trout) and 11 May 2022 (daytime benthic invertebrates releases). After completing the bounding box extraction, drift events containing organisms from these experiments were sorted into the following classes: Heptageniidae, Baetidae, Perlodidae, Capniidae, Rhyacophilidae and *Salmo trutta*. Annotation was performed using Label Studio (Tkachenko et al., 2020). Additionally, several bounding boxes revealed the presence of true fly (Diptera) larvae. Although Diptera larvae were not preserved for taxonomic classification, we included this class in the machine-learning classification, with their identity determined based on visual inspection of the images themselves. The overall dataset contained 4598 bounding boxes from 285 induced drift events distributed among the seven classes (Figure 4a; Figure S9). The machine-learning classification was performed in Python 3.9 (Python Software Foundation, <https://www.python.org/>) using PyTorch (Paszke et al., 2019) and Scikit-learn libraries (Pedregosa et al., 2011).

The Res-Net18 architecture (He et al., 2016), a deep convolutional neural network with 18 deep layers, was used for classification. Non-overlapping cross-validation datasets were created, each containing training (~55%), test (~25%) and validation (~20%) drift events. The unique identifier for each drift event was used as a grouping variable, ensuring that each drift event occurred only once in a test set across all cross-validation

FIGURE 2 Overview of the Riverine Organism Drift Imager (RODI) data acquisition and bounding box extraction. (a) The camera's field of view shows one image of an organism as acquired by RODI. A bounding box is generated for any object or organism within each frame. (b) The sequence of all images acquired for a given organism (shown overlaid on the size of the camera's field of view) is referred to as a 'drift event'. (c) All bounding boxes for each drift event are rescaled to 250×250 pixels for use in the machine-learning classifier.



datasets. Since the image dataset was unevenly distributed among the seven classes, we generated only four unique cross-validation sets to ensure that all seven classes were present in the training, test and validation sets. A Res-Net18 network was trained (AdamW optimiser, learning rate finder and early-stopping activated) for each cross-validation set using its training and validation drift events. This resulted in an array of model weights that were subsequently used to perform classification on the test set drift events for that cross-validation dataset. Since each drift event generated multiple bounding boxes, probabilistic image augmentation techniques were applied to the drift events used for training to prevent model overfitting (Shorten & Khoshgoftaar, 2019). The classification of test set drift events was repeated for each cross-validation dataset, using the respective model weights for each dataset. Classification results were aggregated as each test set was unique and represented ~25% of the complete image dataset. Finally, since each drift event was classified a number of times equal to the number of

bounding boxes in that drift event, the label predicted most frequently was taken as the final label.

Classic machine-learning performance metrics, including precision, recall and the F1 score (Manning et al., 2008; Chapter 8.3), were calculated for each class. Precision is the fraction of true positive classifications among all positive classifications (true and false) for a given class. Recall is the fraction of true positive classifications among all classifications (positive and negative) for a given class. The F1 score of a given class is the harmonic mean of precision and recall for that class. From these scores, we computed a weighted precision, a weighted recall and a weighted F1 score as overall performance metrics suitable for datasets with unbalanced class distributions. Each weighted metric is calculated as the sum of that metric over all classes, where the sum is weighted for each class by the support for that class, that is the proportion of all drift events belonging to that class (Table S1: Proportion of drift events). A confusion matrix was generated to provide insights into the types of misclassification. The code for the machine-learning classifier can be found in Appendix S1.7.



FIGURE 3 Example of bounding boxes (resized to 250×250 pixels) for each of the seven classes used in the machine-learning classification presented in this work. Each bounding box represents one image from one drift event (i.e. each bounding box is a unique organism), and an individual scale bar was added for illustration. The length of the scale bar is fixed on a per-class basis and is thus an approximation that does not account for the water-magnification effect.

To ensure that the applied machine-learning classifier was the suitable approach to our dataset, we performed a principal component analysis (PCA; Jolliffe, 2002) followed by a density-based spatial clustering of applications (DBSCAN; Schubert et al., 2017) on the annotated image dataset (Appendix S1.8: PCA and unsupervised clustering). These techniques were not able to correctly differentiate between the organism classes and instead grouped images according to their raw-pixel value similarities (Figures S7–S9).

2.5 | Natural organism drift at night

Natural drift was measured from 21:00 to 04:10 during the night of 10–11 May 2022 during four measuring intervals, each 1.5 h long. During short time periods between measuring intervals (20–30 min), data were transferred from the laptop to an external hard drive, and the system (drift net and metal fences) was cleaned of debris.

In the images from this experiment, the bounding boxes resulting from image processing were sorted manually, discarding drift events

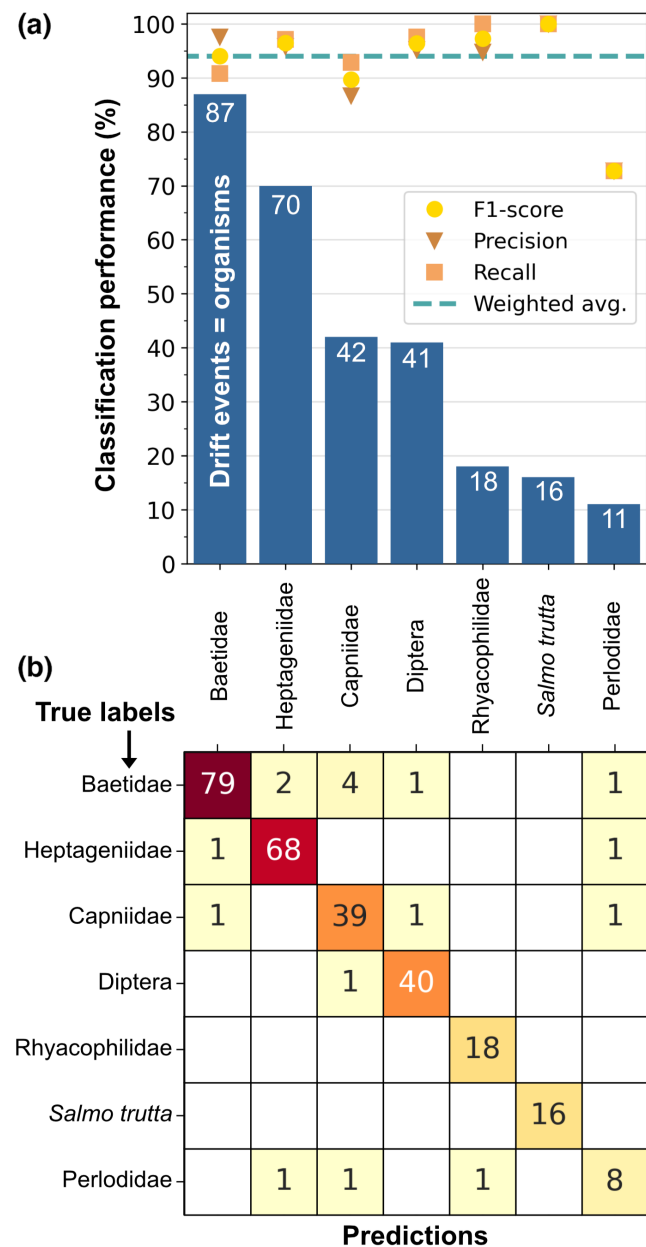


FIGURE 4 Performance of the machine-learning classifier. (a) Classification report, showing, for each of the seven classes on the x-axis, the number of drift events (blue bars; total = 285) and the classification performance (yellow dots = F1 score; brown triangle = precision; orange squares = recall), as well as the performance for the model overall (dashed line = weighted precision, weighted recall and weighted F1 score all equal to 94%). (b) Confusion matrix for the machine-learning classifier, each cell representing a count of classification events. The y-axis represents the true labels, while the x-axis represents the labels predicted by the classifier. A colour gradient represents the value range, from yellow for one to deep red for seventy-nine.

containing debris or bubbles. The remaining drift events were identified by eye into six classes: Ephemeroptera, Plecoptera, Trichoptera, Diptera, Exuviae (discarded exoskeletons after moulting) and non-Benthic-Invertebrates. A unique identifier was assigned to each drift event, along with a time stamp. In these samples, organisms returned

directly to the river environment and were not preserved for laboratory identification. Therefore, taxonomic identification was performed by a human using the bounding boxes, resulting in a lower resolution. During this process, we detected several drifting organisms with different morphologies within the orders Ephemeroptera and Plecoptera that were not present in the annotated dataset used for the machine-learning classifier. As a result, we did not use data from the natural organism drift measurements for the validation of the machine-learning classifier.

3 | RESULTS

3.1 | Device operation

During all deployments, RODI was able to produce continuous sets of images during each acquisition interval without hardware or software issues, and the camera housing remained waterproof even during submersion times of up to 20h. Drift events were recorded equally well during day and night under the flow conditions tested, validating the choice of lighting, camera settings and flow-through dynamics.

Other objects beyond organisms were recorded. Most of the bounding boxes recorded during the natural drift experiment contained debris or bubbles (80%–90%; Figure S10). Debris also clogged the metal fences and drift net, both of which had to be cleaned at the end of each acquisition interval. The high frequency of bubbles and debris was caused by the drift net (40 × 25 cm) projecting above the water surface (water depth, 20 cm) at the deployment site, resulting in the entrainment of air bubbles and debris into the flow tube (Figure 1a,c).

3.2 | Machine-learning classification

The weighted precision, weighted recall and weighted F1 score for the dataset collected on 5 April 2022 and 11 May 2022 (images from both days were aggregated into a single dataset) all had the value of 94% (Figure 4a; Table S1). When considering the classifier's per-class performance (Figure 4a; Table S1), precision, recall and F1 score values ranged between 87% and 100% for all but one class, the Perlodidae. The full details of the inter-class classification performance can be found in the confusion matrix (Figure 4b).

3.3 | Natural organism drift

In total, 674 drifting benthic invertebrates, 254 exuviae and 39 non-benthic invertebrates were imaged during the 6h overnight sampling period from 10 to 11 May. The number of drift events increased as a function of time during the night (grouped in bins of 5 min, Figure 5a and 15 min, Figure 5b). The rate of capture of debris varied during the sampling period, with large amounts of debris that severely

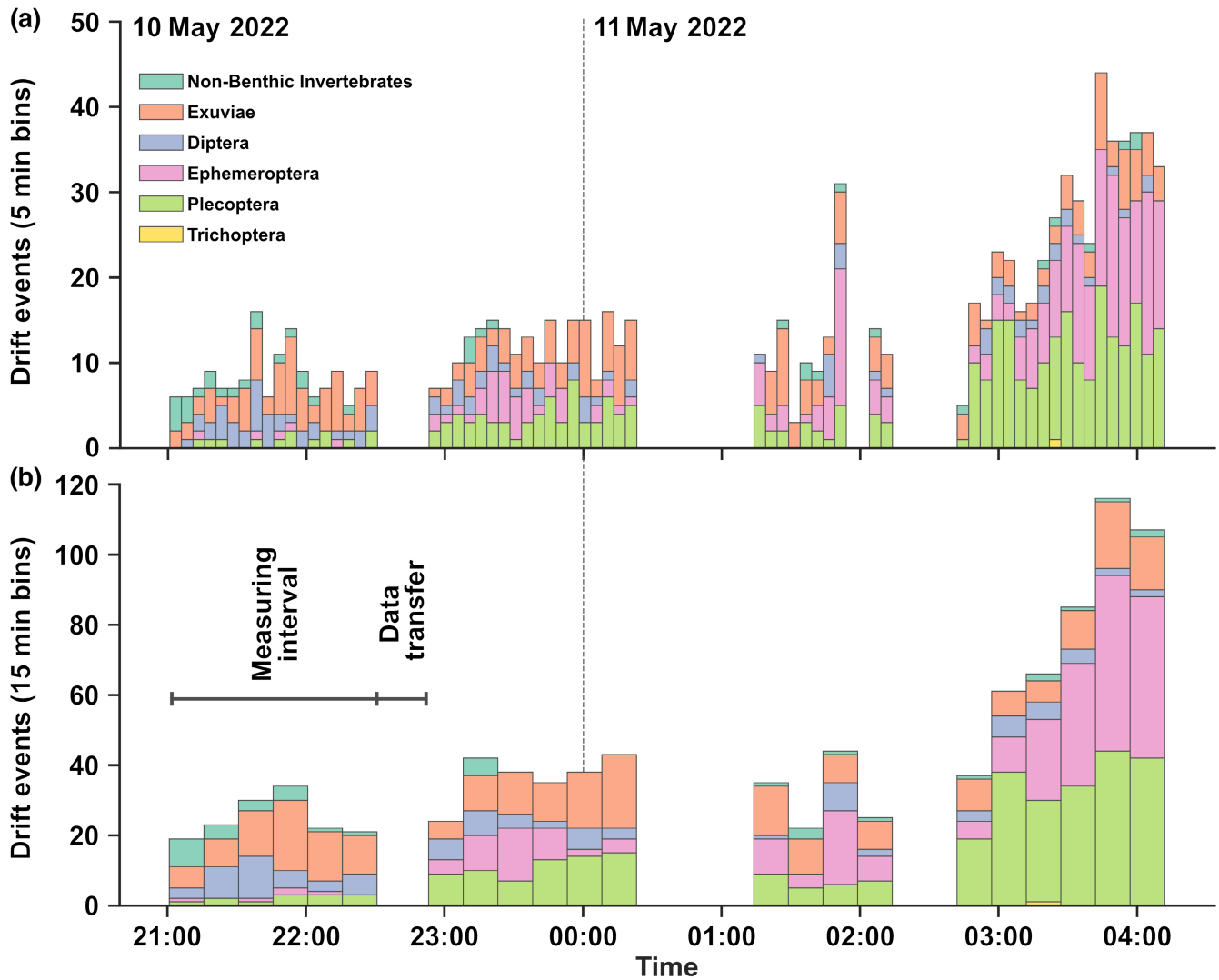


FIGURE 5 Histograms of drifting organisms and exuviae recorded during the night-time deployment. Drifting organisms and exuviae were identified by eye to the order level from images. (a, b) Number of drift events within 5 min (a) and 15 min (b) intervals. Data acquisition intervals lasted 1.5 h, and between intervals, data was transferred (20–30 min) to an external hard drive.

polluted images during the third interval (00:50–01:20). This event severely complicated the bounding box analysis, leading to data loss (Figure S10).

Several patterns could be identified in the distribution of drift events during the night. The total number of drifting invertebrates increased over time, notably the number of Ephemeroptera and Plecoptera. In contrast, the number of drifting Diptera decreased over time. The number of drifting exuviae remained relatively constant, while the number of non-benthic invertebrate drift events decreased. Only one Trichoptera drift event was observed.

4 | DISCUSSION

In this work, we described the technology and first deployments of RODI, an underwater camera system to image drifting organisms, providing a proof of concept for this novel approach. Images of

drifting organisms generated by RODI were of sufficient quality for organisms to be identified to the family level (for benthic invertebrates) using a machine-learning classifier (Figure 4) or to the order level (for all organisms) by a human expert (Figure 5). Here we will discuss the results of the machine-learning classifier and natural organism drift experiments in more detail, highlight current limitations and planned developments to the system, and explore potential scientific and monitoring applications.

4.1 | Machine-learning classifier

The initial application of a machine-learning classifier to identify in situ imaged drifting organisms to the family level had an overall weighted F1 score of 94% (Figure 4a). This result was achieved despite the fact that the classifier had to deal with unevenly distributed drift events between classes, from as few as 11 events (Perlodidae)

to as many as 87 events (Baetidae). The unbalancedness and size of the dataset is a result of the community structure at the sampling site. Perlodidae was the only class with a lower performance (precision, recall and F1 score all equal to 73%), which was most likely due to the limited number of organisms (11) sampled for this class.

Out of 285 drift events, 17 were wrongly classified within the classes of Baetidae, Capniidae, Diptera, Heptageniidae and Perlodidae (Figure 4b). Morphological similarities between these classes and a low number of Perlodidae replicates were the major causes for classification errors (Ärje et al., 2020). Morphologically very distinct classes—Rhyacophilidae and *Salmo trutta*—were perfectly classified.

While the involved taxa are not the same and, thus, the results are not directly comparable, the machine-learning performance presented here is similar to that achieved for preserved benthic invertebrates (Raitoharju et al., 2018) and insects (Bjerger et al., 2021, 2022). Albeit, RODI, in this early implementation, was applied to a lower taxonomic resolution (i.e. family level).

4.2 | Natural organism drift

Although we experienced some issues such as clogging, which are discussed below, capturing natural organism drift at night with this novel approach was straightforward and resulted in data of high temporal resolution. The drift of Ephemeroptera and Plecoptera increased with time, peaking at 04:00 during the night. The drift of these taxa is known to take place predominantly at night as a mechanism to avoid predation during dispersal (Brittain & Eikeland, 1988). The drift of Diptera decreased over time during the night, which corresponds with observations that certain Dipteran families, such as Simuliidae, peak at dusk (Adler et al., 1983; Tilley, 1989). Finally, non-benthic invertebrate drift decreased over time, most likely due to a decreased activity of day-active invertebrates (Waters, 1965). Overall, these results provide a glimpse of the data that could be captured using RODI and underline the potential for studying organism drift with higher temporal resolution.

4.3 | Current limitations and planned developments

In this work, RODI captured organism drift in acquisition intervals of 1.5 h, determined by the hard-drive capacity of the laptop. This limitation did not prevent longer deployments, only resulting in short interruptions between acquisition intervals, yet required human intervention over the entire period of deployment. This bottleneck can be removed by using a higher-capacity computer or, more effectively, by implementing the bounding box analysis in real-time, thereby only saving bounding boxes and not full images. As a result, we expect to reduce the data volume by a factor of around 200, thus enabling continuous sampling of organism drift for nearly 2 weeks using the same hard drive capacity (1 Tb) tested here. Going further,

bounding boxes could be continuously uploaded to a server (if an internet connection were integrated), thereby removing this limitation entirely. In this case, the classifier could automatically identify organisms. This relatively simple improvement would allow RODI to generate real-time data and, ultimately, even to adapt the acquisition campaign based on the generated data.

The smallest object, that is, debris, detected by the bounding box analysis measured approximately 1.5 mm in size, an estimation that does not account for the water magnification effect. A lower area threshold during the bounding box analysis would solve this issue at the cost of many more bounding boxes of debris. Alternatively, the image resolution can be increased by changing the optical train, with the trade-off of generating larger images and thus a greater computational burden. That said, we do not expect many benthic invertebrates and small-bodied fish that do engage in drift to be smaller than 1.5 mm in size (Dodrill et al., 2016; Sandlund, 1982).

A second factor that limited deployment time was clogging of the drift net and metal fences. The fact that RODI was installed downstream of the two metal fences exacerbated the problem of clogging since the fences funnelled debris into the drift net and camera housing. The metal fences were installed to maximise the chances of images drifting organisms, and will be omitted in future deployments. Clogging of the system also likely changed the upstream hydraulic conditions over time. While the many debris objects (and air bubbles) increased the time needed to curate the data, they did not hamper the acquisition of reliable images of organisms for the majority of the deployments. Engineering solutions to prevent clogging are being devised and will include a combination of an upstream filter grid and the replacement of the drift net with a funnel system that should guide debris through the device, instead of getting stuck in the net. This improvement will reduce the need for regular checks during deployments and entrain less debris in the imaging pathway, reducing the number of bounding boxes, hence increasing deployment times.

Although the initial machine-learning results are promising, we expect that system optimisations will produce higher-quality images, which—together with the collection of larger amounts of training data—will bring genus or even species-level identification within reach. Yet, classification to the family level may be sufficient for many applications. For example, monitoring programs using benthic invertebrates as bio-indicators commonly use family-level taxonomical identification (Cortes et al., 2013). A priority development to improve the machine-learning classifier's performance would be the inclusion of organism size as a training parameter. This improvement will help with the distinction of very similar-looking taxa that vary significantly in body size (e.g. Perlodidae and Capniidae). Further improvements of the classifier will be the inclusion of debris, exuviae and air bubbles in the classification scheme to achieve complete automation.

Currently, the data from RODI represents absolute numbers of drifting organisms sampled over a given time interval (Figure S1). For a comparison of organism drift among different conditions and locations, drift densities (individuals m^{-3}) or rates (individuals $m^{-3} s^{-1}$)

have to be estimated (Elliott, 1970). By installing a flow sensor into the system, we can measure the volume of water sampled by the camera, which is determined by the net or funnel area and the flow discharge. Adding additional sensors for temperature, light intensity and turbidity could also be valuable, depending on the application.

Tests in varying turbidity conditions have not been performed. Therefore, it is currently unknown under what levels of turbidity the image quality and classification performance would start to deteriorate substantially. We acknowledge that if the turbidity exceeds a certain threshold, the machine-learning classifier will most likely not be able to recognise drifting organisms in its current implementation. However, RODI images only 5 cm of water with a highly contrasting white background, which should reduce the effect of turbidity during image acquisition. Moreover, with a combination of increased training data on both organisms and debris of different origins, and data augmentation techniques mimicking turbidity conditions, machine learning is expected to be effective even with substantially cluttered images (Noh et al., 2019; Shorten & Khoshgoftaar, 2019). Future experiments will be performed to systematically vary the level of turbidity and assess the degradation in imaging and classification performance.

A further unknown scenario for the application of RODI is the case of very high flow velocity conditions. These can occur during floods, resulting from heavy rain or hydropeaking, the release of water from reservoirs used for hydropower to increase electricity production at peak demand (Bratrich et al., 2004). Very high velocity conditions will pose a double challenge: first, on the operational reliability of RODI's structure (its anchoring, shielding from large debris, maintenance of a stable drift net and level of streamlining of its shape); second, on the quality of the images, as velocities much higher than 2 ms^{-1} could result in image blur. Deployments in high-flow discharge regimes will allow us to explore the limits at which the system can operate and engineer improvements for reliable operation and imaging.

Finally, current deployments have been performed using the power grid. We plan to design a standalone power supply based on a combination of renewable energy, such as solar or small water turbine, and battery storage. This improvement will allow RODI to be deployed in remote locations.

4.4 | Potential applications of RODI in science and monitoring

Despite numerous studies on benthic invertebrate drift (Brittain & Eikeland, 1988; Naman et al., 2016), data on drifting invertebrates remains limited in temporal resolution and scale. The ability to generate data at a high temporal resolution over long deployment times, with only modest labour, has the potential to fill this gap. This also applies to the study of fish larval drift, a crucial process in their life cycle to disperse from nursery to rearing habitats. For example, although many studies have investigated fish larval drift (Lechner et al., 2014, 2018), little is known about the navigation and

motion capacity of larvae during drift (e.g. their ability to orientate and to use active-passive drift mode; Lechner et al., 2016; Pavlov & Mikheev, 2017). The images produced by RODI could help shed light on this and similar questions by providing information on the orientation of drifting fish larvae. For example, larvae drifting with a downstream orientation and a drift velocity exceeding the local current would indicate active rather than passive drift (Lechner et al., 2016). An additional area of application is the study of how drifting organisms cope with the fast-changing conditions associated with hydropeaking events. Hydropeaking is known to induce the drift of riverine organisms (Schülting et al., 2019; Tonolla et al., 2022) and can cause fish mortality due to stranding events when the flow recedes (Schmutz et al., 2015).

Besides the generation of fundamental knowledge on the drift of riverine organisms, RODI holds great potential as a monitoring tool. Many countries currently incentivise hydropower mitigation measures or river restoration projects to reverse the decline in freshwater biodiversity. It is beneficial to precede and follow up these initiatives with long-term impact analyses, including monitoring of aquatic organisms. Tools such as RODI make this monitoring more achievable: one such device can monitor a given location for extended periods of time, while multiple devices can provide spatial resolution; their operation is non-invasive for the organisms being monitored; and the overall effort is substantially reduced in comparison with traditional, drift net-based sampling, rendering monitoring more cost-effective.

5 | CONCLUDING REMARKS

This work demonstrated the viability of RODI, an in situ imaging-based system, to quantify riverine organism drift through the use of a machine-learning classifier to taxonomically identify drifting organisms from images. The machine-learning classifier showed good performance when applied to the drifting community of a river in Switzerland. Future deployments will enrich the dataset available for training, testing and validation, expanding the range of organisms that can be classified and further improving the performance of the machine-learning classifier. Based on this foundation, improvements in automation, hardware and device operation are close at hand. With their implementation, RODI will be ready for expanded use in both scientific studies and biodiversity monitoring, ultimately contributing to effective river and stream management strategies.

AUTHOR CONTRIBUTIONS

Frédéric de Schaetzen, Luiz G. M. Silva and Roman Stocker conceived the idea of RODI. Frédéric de Schaetzen, Patryk Nienaltowski, Michael Arnold, Martin Huber, Luiz G. M. Silva and Roman Stocker contributed to RODI's design and construction. Mikko Impiö and Jenni Raitoharju designed the machine-learning approach. Frédéric de Schaetzen, Basil Wagner, Matthias Meyer and Luiz G. M. Silva performed field deployments and collected data; Frédéric de Schaetzen, Mikko Impiö and Patryk Nienaltowski analysed data;

Frédéric de Schaetzen, Luiz G. M. Silva and Roman Stocker led the writing of the manuscript. All authors contributed to the drafts and gave final approval for publication.

ACKNOWLEDGEMENTS

We thank Kraftwerke Oberhasli for providing us with the ideal conditions to perform RODI deployments; Vicente Fernandez, Nicholas Macias, Jules Jaffe, Christopher Robinson, Daniel Braun, Zachary Landry and colleagues of the Stockerlab for their help and feedback on this project; Anne-Marie Cools and Thomas Meierhans for help with the construction of RODI; and Elzbieta Sliwerska for help with logistics. Lastly, we thank Russel Naisbit for his editorial input.

CONFLICT OF INTEREST STATEMENT

The authors declare no conflicts of interest.

FUNDING INFORMATION

This work did not receive any external funding. It was completely financed by the yearly lab-fund Roman Stocker receives from ETH Zürich.

PEER REVIEW

The peer review history for this article is available at <https://www.webofscience.com/api/gateway/wos/peer-review/10.1111/2041-210X.14130>.

DATA AVAILABILITY STATEMENT

Instructions on the build process, how to operate the Riverine Organism Drift Imager (RODI) and the machine-learning classifier can be found in the [Supporting Information](#) and the following Github link: <https://github.com/FdeSchae/RODI> (<https://doi.org/10.5281/zenodo.7906641>; de Schaetzen et al., 2023). The annotated image dataset used for the machine-learning classification can be found at: <https://kaggle.com/datasets/073b9a4e5d84c514ca7806df918e09cd35c0c285f28d8dcc93190f26fefecd8a>; and the image dataset resulting from the natural organism drift can be found at: <https://kaggle.com/datasets/54e0e9bc6cc437ec8d77e0f1cce45d47e7e326355c9a8ed09c3e82bc24f6e26>. The raw data recorded in this work is too large (~10Tb) to be sustainably shared through a cloud server and is available upon request.

ORCID

Frédéric de Schaetzen  <https://orcid.org/0000-0002-9309-4274>

Mikko Impiö  <https://orcid.org/0000-0001-7672-3000>

Patryk Nienaltowski  <https://orcid.org/0000-0003-2308-9450>

Jenni Raitoharju  <https://orcid.org/0000-0003-4631-9298>

Luiz G. M. Silva  <https://orcid.org/0000-0002-2329-5601>

Roman Stocker  <https://orcid.org/0000-0002-3199-0508>

REFERENCES

- Adler, P. H., Light, R. W., & Kim, K. C. (1983). The aquatic drift patterns of black flies (Diptera: Simuliidae). *Hydrobiologia*, 107(2), 183–191. <https://doi.org/10.1007/BF00017433>

- Albert, J. S., Destouni, G., Duke-Sylvester, S. M., Magurran, A. E., Oberdorff, T., Reis, R. E., Winemiller, K. O., & Ripple, W. J. (2021). Scientists' warning to humanity on the freshwater biodiversity crisis. *Ambio*, 50(1), 85–94. <https://doi.org/10.1007/S13280-020-01318-8>
- Ärje, J., Melvad, C., Jeppesen, M. R., Madsen, S. A., Raitoharju, J., Rasmussen, M. S., Iosifidis, A., Tirronen, V., Gabbouj, M., Meissner, K., & Høye, T. T. (2020). Automatic image-based identification and biomass estimation of invertebrates. *Methods in Ecology and Evolution*, 11(8), 922–931. <https://doi.org/10.1111/2041-210X.13428>
- Bauernfeind, E., & Humpesch, U. H. (2001). *Die Eintagsfliegen Zentraleuropas (Insecta: Ephemeroptera) Bestimmung und Ökologie*. Verlag des Naturhistorischen Museums Wien.
- Bjerge, K., Mann, H. M. R., & Høye, T. T. (2022). Real-time insect tracking and monitoring with computer vision and deep learning. *Remote Sensing in Ecology and Conservation*, 8(3), 315–327. <https://doi.org/10.1002/RSE2.245>
- Bjerge, K., Nielsen, J. B., Sepstrup, M. V., Helsing-Nielsen, F., & Høye, T. T. (2021). An automated light trap to monitor moths (Lepidoptera) using computer vision-based tracking and deep learning. *Sensors*, 21(2), 343. <https://doi.org/10.3390/S21020343>
- Bradski, G. (2000). *The OpenCV library*. Dr. Dobb's Journal of Software Tools.
- Bratrich, C., Truffer, B., Jorde, K., Markard, J., Meier, W., Peter, A., Schneider, M., & Wehrli, B. (2004). Green hydropower: A new assessment procedure for river management. *River Research and Applications*, 20(7), 865–882. <https://doi.org/10.1002/RRA.788>
- Brittain, J. E., & Eikeland, T. J. (1988). Invertebrate drift? A review. *Hydrobiologia*, 166(1), 77–93. <https://doi.org/10.1007/BF00017485>
- Castañeda, R. A., Van Nynatten, A., Crookes, S., Ellender, B. R., Heath, D. D., Maclsaac, H. J., Mandrak, N. E., & Weyl, O. L. F. (2020). Detecting native freshwater fishes using novel non-invasive methods. *Frontiers in Environmental Science*, 8, 29. <https://doi.org/10.3389/FENV.2020.00029>
- Cortes, R. M. V., Hughes, S. J., Pereira, V. R., & Varandas, S. D. G. P. (2013). Tools for bioindicator assessment in rivers: The importance of spatial scale, land use patterns and biotic integration. *Ecological Indicators*, 34, 460–477. <https://doi.org/10.1016/J.ECOLI.2013.06.004>
- de Schaetzen, F., Impiö, M., Wagner, B., Nienaltowski, P., Arnold, M., Huber, M., Meyer, M., Raitoharju, J., Silva, L. G. M., & Stocker, R. (2023). Data from: The Riverine Organism Drift Imager (RODI): A new technology to study organism drift in rivers and streams. Zenodo <https://doi.org/10.5281/zenodo.7906641>
- Deinet, S., Scott-Gatty, K., Rotton, H., Twardek, W. M., Marconi, V., McRae, L., Baumgartner, L. J., Brink, K., Claussen, J. E., Cooke, S. J., Darwall, W., Eriksson, B. K., Garcia de Leaniz, C., Hogan, Z., Royte, J., Silva, L. G. M., Thieme, M. L., Tickner, D., Waldman, J., ... Berkhuyzen, A. (2020). *The Living Planet Index (LPI) for migratory freshwater fish—Technical report*. <https://worldfishmigrationfoundation.com/living-planet-index-2020/>
- Dodrill, M. J., Yackulic, C. B., Kennedy, T. A., & Hayes, J. W. (2016). Prey size and availability limits maximum size of rainbow trout in a large tailwater: Insights from a drift-foraging bioenergetics model. *Canadian Journal of Fisheries and Aquatic Sciences*, 73(5), 759–772. <https://doi.org/10.1139/CJFAS-2015-0268>
- Elliott, J. M. (1970). Methods of sampling invertebrate drift in running water. *Annales de Limnologie—International Journal of Limnology*, 6(2), 133–159. <https://doi.org/10.1051/LIMN/1970017>
- FOEN. (2022). *Gewässer in der Schweiz*. Zustand und Massnahmen.
- Franciscangeli, M., Marini, S., Martínez, E., Del Río, J., Toma, D. M., Noguera, M., & Aguzzi, J. (2023). Image dataset for benchmarking automated fish detection and classification algorithms. *Scientific Data*, 10(1), 1–13. <https://doi.org/10.1038/s41597-022-01906-1>

- Grossman, G. D. (2014). Not all drift feeders are trout: A short review of fitness-based habitat selection models for fishes. *Environmental Biology of Fishes*, 97(5), 465–473. <https://doi.org/10.1007/s10641-013-0198-3>
- He, K., Zhang, X., Ren, S., & Sun, J. (2016). Deep residual learning for image recognition. *Proceedings of the IEEE computer society conference on computer vision and pattern recognition, 2016-December*, pp. 770–778. <https://doi.org/10.1109/CVPR.2016.90>
- Holter, T. H., Myrvold, K. M., Pulg, U., & Museth, J. (2020). Evaluating a fishway reconstruction amidst fluctuating abundances. *River Research and Applications*, 36(8), 1748–1753. <https://doi.org/10.1002/RRA.3688>
- Hopkins, G. W., & Freckleton, R. P. (2002). Declines in the numbers of amateur and professional taxonomists: Implications for conservation. *Animal Conservation*, 5(3), 245–249. <https://doi.org/10.1017/S1367943002002299>
- Høyte, T. T., Ärje, J., Bjerger, K., Hansen, O. L. P., Iosifidis, A., Leese, F., Mann, H. M. R., Meissner, K., Melvad, C., & Raitoharju, J. (2021). Deep learning and computer vision will transform entomology. *Proceedings of the National Academy of Sciences of the United States of America*, 118(2), e2002545117. <https://doi.org/10.1073/PNAS.2002545117>
- Høyte, T. T., Dyrmann, M., Kjær, C., Nielsen, J., Bruus, M., Mielec, C. L., Vesterdal, M. S., Bjerger, K., Madsen, S. A., Jeppesen, M. R., & Melvad, C. (2022). Accurate image-based identification of macroinvertebrate specimens using deep learning—How much training data is needed? *PeerJ*, 10, e13837. <https://doi.org/10.7717/PEERJ.13837>
- Humphries, P., King, A., McCasker, N., Kopf, R. K., Stoffels, R., Zampatti, B., & Price, A. (2020). Riverscape recruitment: A conceptual synthesis of drivers of fish recruitment in rivers. *Canadian Journal of Fisheries and Aquatic Sciences*, 77(2), 213–225. <https://doi.org/10.1139/CJFAS-2018-0138>
- Jolliffe, I. T. (2002). *Principal component analysis*. Springer. <https://doi.org/10.1007/b98835>
- Lechner, A., Keckeis, H., Glas, M., Tritthart, M., Habersack, H., Andorfer, L., & Humphries, P. (2018). The influence of discharge, current speed, and development on the downstream dispersal of larval nase (*Chondrostoma nasus*) in the River Danube. *Canadian Journal of Fisheries and Aquatic Sciences*, 75(2), 247–259. <https://doi.org/10.1139/CJFAS-2016-0340>
- Lechner, A., Keckeis, H., & Humphries, P. (2016). Patterns and processes in the drift of early developmental stages of fish in rivers: A review. *Reviews in Fish Biology and Fisheries*, 26(3), 471–489. <https://doi.org/10.1007/s11160-016-9437-y>
- Lechner, A., Keckeis, H., Schludermann, E., Humphries, P., McCasker, N., & Tritthart, M. (2014). Hydraulic forces impact larval fish drift in the free flowing section of a large European river. *Ecohydrology*, 7(2), 648–658. <https://doi.org/10.1002/ECO.1386>
- Lürig, M. D., Donoughe, S., Svensson, E. I., Porto, A., & Tsuboi, M. (2021). Computer vision, machine learning, and the promise of phenomics in ecology and evolutionary biology. *Frontiers in Ecology and Evolution*, 9, 148. <https://doi.org/10.3389/FEVO.2021.642774>
- Lytle, D. A., Martínez-Muñoz, G., Zhang, W., Larios, N., Shapiro, L., Paasch, R., Moldenke, A., Mortensen, E. N., Todorovic, S., & Dietterich, T. G. (2010). Automated processing and identification of benthic invertebrate samples. *Journal of the North American Benthological Society*, 29(3), 867–874. <https://doi.org/10.1899/09-080.1>
- Manning, C. D., Raghavan, P., & Schütze, H. (2008). Evaluation in information retrieval. In *Introduction to information retrieval*. Cambridge University Press. <https://doi.org/10.1017/CBO9780511809071>
- Meyer, M., Greter, R., Schweizer, S., Baumgartner, J., Schläppi, S., & Büsser, P. (2019). *Untersuchungen zum Emergenzzeitraum von Salmo trutta in der Hasliaare in 2018*. Federal Office for the Environment.
- Naman, S. M., Rosenfeld, J. S., & Richardson, J. S. (2016). Causes and consequences of invertebrate drift in running waters: From individuals to populations and trophic fluxes. *Canadian Journal of Fisheries and Aquatic Sciences*, 73(8), 1292–1305. <https://doi.org/10.1139/cjfas-2015-0363>
- Noh, J. M., Jang, G. R., Ha, K. N., & Park, J. H. (2019). *Data augmentation method for object detection in underwater environments*. In International conference on control, automation and systems, 2019-October, pp. 324–328. <https://doi.org/10.23919/ICCAS47443.2019.8971728>
- Paszke, A., Gross, S., Massa, F., Lerer, A., Bradbury, J., Chanan, G., Killeen, T., Lin, Z., Gimelshein, N., Antiga, L., Desmaison, A., Köpf, A., Yang, E., DeVito, Z., Raison, M., Tejani, A., Chilamkurthy, S., Steiner, B., Fang, L., ... Chintala, S. (2019). PyTorch: An imperative style, high-performance deep learning library. *Advances in Neural Information Processing Systems*, 32. <https://doi.org/10.48550/1912.01703>
- Pavlov, D. S. (1994). The downstream migration of young fish in rivers—Mechanisms and distribution. *Folia Zoologica*, 43(3), 193–208.
- Pavlov, D. S., & Mikheev, V. N. (2017). Downstream migration and mechanisms of dispersal of young fish in rivers. *Canadian Journal of Fisheries and Aquatic Sciences*, 74(8), 1312–1323. <https://doi.org/10.1139/cjfas-2016-0298>
- Pedregosa, F., Varoquaux, G., Gramfort, A., Michel, V., Thirion, B., Grisel, O., Blondel, M., Prettenhofer, P., Weiss, R., Dubourg, V., Vanderplas, J., Passos, A., Cournapeau, D., Brucher, M., Perrot, M., & Duchesnay, É. (2011). Scikit-learn: Machine learning in python. *Journal of Machine Learning Research*, 12(85), 2825–2830. <http://jmlr.org/papers/v12/pedregosa11a.html>
- Raitoharju, J., Riabchenko, E., Ahmad, I., Iosifidis, A., Gabbouj, M., Kiranyaz, S., Tirronen, V., Ärje, J., Kärkkäinen, S., & Meissner, K. (2018). Benchmark database for fine-grained image classification of benthic macroinvertebrates. *Image and Vision Computing*, 78, 73–83. <https://doi.org/10.1016/j.imavis.2018.06.005>
- Sandlund, O. T. (1982). The drift of zooplankton and microzoobenthos in the river Strandaelva, western Norway. *Hydrobiologia*, 94(1), 33–48. <https://doi.org/10.1007/BF00008632>
- Schindelin, J., Arganda-Carreras, I., Frise, E., Kaynig, V., Longair, M., Pietzsch, T., Preibisch, S., Rueden, C., Saalfeld, S., Schmid, B., Tinevez, J. Y., White, D. J., Hartenstein, V., Eliceiri, K., Tomancak, P., & Cardona, A. (2012). Fiji: An open-source platform for biological-image analysis. *Nature Methods*, 9(7), 676–682. <https://doi.org/10.1038/nmeth.1919>
- Schmutz, S., Bakken, T. H., Friedrich, T., Greimel, F., Harby, A., Jungwirth, M., Melcher, A., Unfer, G., & Zeiringer, B. (2015). Response of fish communities to hydrological and morphological alterations in hydropeaking Rivers of Austria. *River Research and Applications*, 31(8), 919–930. <https://doi.org/10.1002/RRA.2795>
- Schubert, E., Sander, J., Ester, M., Kriegel, H. P., & Xu, X. (2017). DBSCAN revisited, revisited: Why and how you should (still) use DBSCAN. *ACM Transactions on Database Systems (TODS)*, 42(3), 1–21. <https://doi.org/10.1145/3068335>
- Schülting, L., Feld, C. K., Zeiringer, B., Hudek, H., & Graf, W. (2019). Macroinvertebrate drift response to hydropeaking: An experimental approach to assess the effect of varying ramping velocities. *Ecohydrology*, 12(1). <https://doi.org/10.1002/ECO.2032>
- Schweizer, S., Meyer, M., Wagner, T., & Weissmann, H. Z. (2012). *Gewässerökologische Aufwertungen im Rahmen der Restwassersanierung und Ausbauvorhaben an der Grimsel*. Wasser Energie Luft.
- Shorten, C., & Khoshgoftaar, T. M. (2019). A survey on image data augmentation for deep learning. *Journal of Big Data*, 6(1), 1–48. <https://doi.org/10.1186/S40537-019-0197-0>
- Struthers, D. P., Danylchuk, A. J., Wilson, A. D. M., & Cooke, S. J. (2015). Action cameras: Bringing aquatic and fisheries research into view. *Fisheries*, 40(10), 502–512. <https://doi.org/10.1080/03632415.2015.1082472>
- Tilley, L. J. (1989). Diel drift of Chironomidae larvae in a pristine Idaho mountain stream. *Hydrobiologia*, 174(2), 133–149. <https://doi.org/10.1007/BF00014061>

- Tkachenko, M., Malyuk, M., Holmanyuk, A., & Liubimov, N. (2020). *Label studio: Data labeling software*. <https://github.com/heartexlabs/label-studio>
- Tonolla, D., Dossi, F., Kastenhofer, O., Doering, M., Hauer, C., Graf, W., & Schülting, L. (2022). Effects of hydropeaking on drift, stranding and community composition of macroinvertebrates: A field experimental approach in three regulated Swiss rivers. *River Research and Applications*, 39, 427–443. <https://doi.org/10.1002/RRA.4019>
- Waringer, J., & Graf, W. (2013). Key and bibliography of the genera of European Trichoptera larvae. *Zootaxa*, 3640(2), 101–151. <https://doi.org/10.11646/ZOOTAXA.3640.2.1>
- Waters, T. F. (1965). Interpretation of invertebrate drift in streams. *Ecology*, 46(3), 327–334. <https://doi.org/10.2307/1936336>
- Zwerts, J. A., Stephenson, P. J., Maisels, F., Rowcliffe, M., Astaras, C., Jansen, P. A., van der Waarde, J., Sterck, L. E. H. M., Verweij, P. A., Bruce, T., Brittain, S., & van Kuijk, M. (2021). Methods for wildlife monitoring in tropical forests: Comparing human observations, camera traps, and passive acoustic sensors. *Conservation Science and Practice*, 3(12), e568. <https://doi.org/10.1111/CSP2.568>
- Zwick, P. (2004). Key to the west palaeartic genera of stoneflies (plecoptera) in the larval stage. *Limnologica*, 34(4), 315–348. [https://doi.org/10.1016/S0075-9511\(04\)80004-5](https://doi.org/10.1016/S0075-9511(04)80004-5)

SUPPORTING INFORMATION

Additional supporting information can be found online in the Supporting Information section at the end of this article.

Appendix S1. Technology description.

How to cite this article: de Schaetzen, F., Impiö, M., Wagner, B., Nienaltowski, P., Arnold, M., Huber, M., Meyer, M., Raitoharju, J., Silva, L. G. M., & Stocker, R. (2023). The Riverine Organism Drift Imager: A new technology to study organism drift in rivers and streams. *Methods in Ecology and Evolution*, 00, 1–13. <https://doi.org/10.1111/2041-210X.14130>